

# Chromatin configuration and epigenetic landscape at the sex chromosome bivalent during equine spermatogenesis

Claudia Baumann · Christopher M. Daly ·  
Sue M. McDonnell · Maria M. Viveiros ·  
Rabindranath De La Fuente

Received: 24 May 2010 / Revised: 3 December 2010 / Accepted: 16 December 2010 / Published online: 28 January 2011  
© Springer-Verlag 2010

**Abstract** Pairing of the sex chromosomes during mammalian meiosis is characterized by the formation of a unique heterochromatin structure at the XY body. The mechanisms underlying the formation of this nuclear domain are reportedly highly conserved from marsupials to mammals. In this study, we demonstrate that in contrast to all eutherian species studied

to date, partial synapsis of the heterologous sex chromosomes during pachytene stage in the horse is not associated with the formation of a typical macrochromatin domain at the XY body. While phosphorylated histone H2AX ( $\gamma$ H2AX) and macroH2A1.2 are present as a diffuse signal over the entire macrochromatin domain in mouse pachytene spermatocytes,  $\gamma$ H2AX, macroH2A1.2, and the cohesin subunit SMC3 are preferentially enriched at meiotic sex chromosome cores in equine spermatocytes. Moreover, although several histone modifications associated with this nuclear domain in the mouse such as H3K4me2 and ubH2A are conspicuously absent in the equine XY body, prominent RNA polymerase II foci persist at the sex chromosomes. Thus, the localization of key marker proteins and histone modifications associated with the XY body in the horse differs significantly from all other mammalian systems described. These results demonstrate that the epigenetic landscape and heterochromatinization of the equine XY body might be regulated by alternative mechanisms and that some features of XY body formation may be evolutionary divergent in the domestic horse. We propose equine spermatogenesis as a unique model system for the study of the regulatory networks leading to the epigenetic control of gene expression during XY body formation.

Communicated by S. Keeney

**Electronic supplementary material** The online version of this article (doi:10.1007/s00412-010-0306-5) contains supplementary material, which is available to authorized users.

C. Baumann · R. De La Fuente  
Female Germ Cell Biology Group, Department of Clinical Studies, University of Pennsylvania, New Bolton Center, 382 West Street Road, Kennett Square, PA 19348, USA

C. M. Daly · M. M. Viveiros  
Department of Animal Biology, Center for Animal Transgenesis and Germ Cell Research, University of Pennsylvania, New Bolton Center, 382 West Street Road, Kennett Square, PA 19348, USA

C. Baumann · S. M. McDonnell · R. De La Fuente  
Section of Reproduction, Department of Clinical Studies, School of Veterinary Medicine, University of Pennsylvania, New Bolton Center, 382 West Street Road, Kennett Square, PA 19348, USA

C. Baumann · M. M. Viveiros (✉) · R. De La Fuente (✉)  
Department of Physiology and Pharmacology, College of Veterinary Medicine, University of Georgia, 501 D.W. Brooks Drive, Athens, GA 30605, USA  
e-mail: viveiros@uga.edu

R. De La Fuente  
e-mail: rfuelle@uga.edu

## Introduction

Homologous chromosome synapsis is essential for the formation of reciprocal recombination sites as well as proper chromosome segregation (Burgoyne et al. 2009). In direct contrast with the process of autosomal chromosome synapsis, differences in size and DNA sequence result in partial synapsis between heterologous sex chromosomes in mammals (Zickler 2006; Turner 2007) such that pairing of the X and Y chromosomes is restricted to a limited segment of

sequence homology, the pseudoautosomal region (PAR) (Handel and Hunt 1992; Perry et al. 2001). Partial synapsis between sex chromosomes is associated with the initiation of a unique process known as meiotic sex chromosome inactivation (MSCI) which involves large-scale chromatin remodeling as well as recruitment of key nuclear factors for the formation of a transcriptionally silenced, morphologically distinct nuclear domain: the XY body (Handel 2004; Turner et al. 2006; Turner 2007). Although MSCI occurs in the germ line of nearly all organisms with heteromorphic sex chromosomes (Namekawa and Lee 2009), the underlying epigenetic mechanisms of XY body formation in mammals are not fully understood. Comparative studies of MSCI in several species, however, have provided critical insight into the potential role of different XY marker proteins and their functional implications for transcriptional silencing, chromatin remodeling, and the process of heterochromatinization of this large nuclear domain (Fernandez-Capetillo et al. 2003; Hoyer-Fender 2003; Page et al. 2003; Namekawa and Lee 2009).

Targeted deletion of the histone variant H2AX resulted in the initial identification of a critical chromatin modification that is necessary for the establishment of MSCI in the mammalian male germ line (Fernandez-Capetillo et al. 2003). For example, spermatocytes of mice deficient for H2AX do not form an XY body, exhibit abnormal sex chromosome synapsis, and fail to initiate MSCI, indicating that H2AX and its phosphorylated form ( $\gamma$ H2AX) are crucial for chromatin remodeling and transcriptional silencing of the XY body in male germ cells (Fernandez-Capetillo et al. 2003). Subsequent studies revealed a critical pathway for XY body formation in mouse spermatocytes in which the tumor suppressor gene BRCA1 is required to recruit the ATR kinase to the sex chromosomes, which in turn directs the accumulation of  $\gamma$ H2AX at the XY body during the pachytene stage (Xu et al. 2003; Turner et al. 2004, 2005). Accumulation of  $\gamma$ H2AX at the XY body has also been observed in human (Sciurano et al. 2007) and marsupial (Franco et al. 2007; Namekawa et al. 2007) germ cells suggesting that the pathways leading to MSCI and XY body formation may be evolutionarily conserved (Franco et al. 2007; Namekawa and Lee 2009).

The cohesin subunits, structural maintenance of chromosomes 1 and 3 (SMC1/SMC3), play a critical role in sister chromatid cohesion and DNA recombination (Losada and Hirano 2005; Pelttari et al. 2001). Importantly, both SMC1 and SMC3 establish a physical interaction with the synaptonemal complex proteins SYCP2 and SYCP3 in rat spermatocytes as part of a large protein complex that associates with the axial elements of the synaptonemal complex (Eijpe et al. 2000). Notably, the amino acid sequences of the coiled-coil domains of SMC1/SMC3 proteins are among the most highly conserved proteins in

mammals with an estimated amino acid divergence between the human and mouse proteins of only 1% (White and Erickson 2006) and hence provide a unique experimental paradigm for the analysis of chromatin condensation as well as the dynamics of homologous chromosome synapsis in mammalian species such as the horse in which meiotic marker proteins have not been previously characterized.

In this study, we investigated the process of meiotic sex chromosome inactivation in the equine germ line. Surprisingly, our analysis reveals that several key transcriptionally repressive chromatin modifications, associated with the macrochromatin domain during mouse spermatogenesis, are conspicuously absent from the XY body in equine spermatocytes. Our results indicate, therefore, that the epigenetic landscape at sex chromatin in the horse differs significantly from other mammalian species and suggests some degree of evolutionary divergence in the mechanisms involved in large-scale chromatin remodeling at the sex chromosome bivalent. To our knowledge, this study constitutes the first analysis of the process of XY body formation in the equine germ line.

## Materials and methods

### Animals, testis tissue collection, and preparation of meiotic spreads

Equine testicular tissue was obtained from adult (>2-year-old) males following surgical castration. Tissue samples were dissected in PBS supplemented with 10% fetal calf serum and immediately processed for the analysis of marker proteins of meiotic sex chromosome inactivation and chromosome synapsis on surface spread meiocytes as described previously (De La Fuente et al. 2006). Briefly, seminiferous tubules were subjected to a mild hypotonic treatment by exposure to a 1% sodium citrate solution for 20 to 25 min at room temperature. Germ cells were subsequently spread onto glass slides containing 1% paraformaldehyde and 0.15% Triton X in H<sub>2</sub>O to facilitate nuclear protein cross-linking. Slides were allowed to air dry and stored at  $-80^{\circ}\text{C}$  until further analysis. Mouse testicular germ cell spreads were prepared identically and comparative analyses were always conducted in parallel.

### Immunocytochemistry of chromosomal spreads

The stage of prophase I of meiosis in equine spermatocytes was determined according to the extent of chromosomal synapsis visualized by immunocytochemical detection of the cohesin subunit SMC3 protein at axial/lateral elements of the synaptonemal complex (subsequently referred to as cohesin axes). Pachytene sub-

stages were differentiated by the degree of terminal synapsis of autosomal bivalents from early pachytene to mid- and late pachytene and the transition into diplotene through a diplotene-like appearance (interstitial desynapsis) as well as by the level of pairing of the sex chromosomes. The localization of SMC3 on meiotic chromosomes was detected using a 1:400 dilution of a polyclonal rabbit anti-SMC3 antibody (Abcam, Cambridge, MA, USA). The sub-cellular localization of histone H2A phosphorylated at Serine 139 ( $\gamma$ H2AX) was determined using a mouse anti- $\gamma$ H2AX antibody (Upstate, Charlottesville, VA, USA) at a 1:500 dilution. A rabbit anti-macroH2A1.2 antibody was purchased from Upstate and used at a 1:400 dilution. Human anti-CREST antiserum (1:50,000 dilution; a generous gift from Dr. W. Earnshaw) in combination with anti-SMC3 antibody was used to detect kinetochore domains within centromeric heterochromatin. Anti-H3K4me2 (Upstate) and mouse anti-Smith antigen antibody (Neomarkers, Fremont, CA, USA) were used at a 1:400 dilution. Immunohistochemical detection of DNA repair and recombination associated proteins was conducted using a mouse polyclonal anti-RAD51 (Oncogene) and a mouse monoclonal anti-MLH1 (BD Pharmingen) antibody at a 1:50 dilution, respectively. RNA polymerase II was detected using a 1:200 dilution of a mouse IgG antibody raised against a synthetic peptide (YSPTSpPS) corresponding to the carboxy-terminal repeat domain of human RNA Pol II (Active Motif, Carlsbad, CA, USA), which recognizes both the phosphorylated and unphosphorylated forms of the largest subunit of RNA Pol II. Secondary antibodies were purchased from Molecular Probes (Eugene, OR, USA). Alexa-fluor 488 goat anti-rabbit, Alexa-fluor 555 goat anti-mouse, and Alexa-fluor 555 goat anti-human were used at 1:1,000 or 1:500 dilution, respectively. After immunostaining, slides were counterstained with 8  $\mu$ l of antifading medium supplemented with 4',6'-diamidino-2-phenylindole (DAPI) (Vectashield; Vector Laboratories, Burlingame, CA, USA).

#### Fluorescence in situ hybridization

Following immunohistochemical localization of the SMC3 protein and establishing the patterns of  $\gamma$ H2AX localization at the pachytene stage, the position of the sex chromosome bivalent in equine spermatocytes was determined by fluorescence in situ hybridization (FISH) analysis using Cy3-conjugated equine-specific or mouse-specific X chromosome paints (STARFISH, Cambio), respectively, essentially as described previously (De La Fuente et al. 2004). Briefly, probe denaturation was carried out at 75°C for 10 min, followed by overnight hybridization at 40°C. Stringency washes were conducted in 50% formamide and 2 $\times$  SSC.

#### Analysis of *Smc3* gene expression by RT-PCR

Testis messenger RNA (mRNA) was extracted using a Microfast Track 2.0 kit (Invitrogen) following the manufacturer's instructions and cDNA synthesis was conducted using the SuperScript First-Strand Synthesis System (Invitrogen). The specific PCR conditions were as follows: 94°C for 3 min; 34 cycles of 94°C for 30 s, 54.5°C (*Smc3*) or 57°C ( $\beta$ -actin) for 1 min, and 72°C for 1 min; followed by 72°C for 10 min. The following primer pairs were used: *Smc3*-Fwd, 5'-gca gcg att ggc ttt gtt gc-3'; *Smc3*-Rev, 5'-cca gca ctt tca agg aga ttc atc-3';  $\beta$ -actin-Fwd, 5'-gat atc gct gcg ctg gtc gtc-3';  $\beta$ -actin-Rev, 5'-acg cag ctc att gta gaa ggt gtc g-3' with expected band sizes of 210 and 276 bp, respectively.

#### Non-biased co-localization measurements and quantitative image analysis

Mean fluorescence intensity was determined for 10 representative mouse and 10 horse pachytene spermatocytes. Care was taken to select well-spread nuclei of approximately similar size. Fluorescence intensity of SMC3 staining along the fully synapsed chromosome cores of two randomly selected autosomes and the sex chromosome pair was quantified using the measurements module of Improvision software (Openlab). The signal intensity of the sex bivalent in each nucleus was normalized to the average intensity of two randomly selected autosomal bivalents and expressed as the percent difference in intensity. Non-biased co-localization analysis was conducted using CoLocalizer Pro 2.0 software to calculate the overlap coefficient according to Manders (*R*), which quantifies the degree of overlapping pixels between two channels (i.e., red and green) and is considered to represent a true measure of protein co-localization (Zinchuk and Zinchuk 2008; Zinchuk et al. 2007; Manders et al. 1993). Values ranging between 0.6 and 1.0 represent co-localization of the proteins in question, while values between 0 and 0.6 indicate absence of co-localization. The overlap coefficient according to Manders was calculated for the nuclear domain occupied by  $\gamma$ H2AX in relation to SMC3 after background correction in 10 randomly selected mouse and 10 horse pachytene spermatocytes.

#### Statistical analysis

Data are presented as the mean percentage of at least three independent experiments and variation among replicates is indicated as the standard deviation (SD). Percentage values of individual experiments were analyzed following arcsine transformation and comparison by Student's *t* test using JMP Start Statistics (SAS Institute, Inc., Cary, NC, USA). Differences were considered significant when  $p < 0.05$ .

## Results

### Expression and chromosomal localization of SMC3 in equine spermatocytes

In the majority of mammalian species studied to date, the sex chromosomes undergo a progressive condensation during prophase I of meiosis resulting in the formation of a DAPI-bright, macrochromatin domain (Handel 2004). In contrast, equine pachytene spermatocytes show striking differences in nuclear architecture and large-scale chromatin organization as indicated by a homogeneous DAPI staining pattern associated with nearly indistinguishable euchromatic and heterochromatic domains (Fig. 1). For example, in mouse pachytene spermatocytes, the nuclear

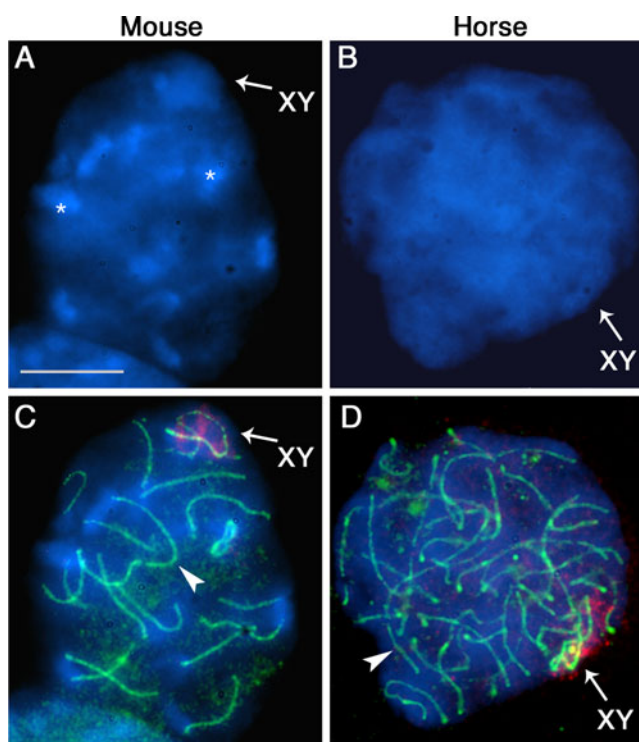


**Fig. 1** Nuclear morphology and cytological appearance of chromatin domains in mouse and horse spermatocyte nuclei indicate major differences in chromatin organization. **a** DAPI-stained pachytene spermatocyte from the mouse. DAPI-bright heterochromatin domains (*asterisks*) are clearly distinguishable from DAPI-pale euchromatic areas. **c** The position of the sex chromosome-containing XY body is distinctly visible by DAPI staining (*arrows* in **a** and **c**) and colocalizes with the signal obtained following *in situ* hybridization (FISH) using an X chromosome-specific probe (*red*). **b** Typical chromatin organization in pachytene spermatocytes from the horse. Heterochromatin and euchromatin domains are indistinguishable by DAPI staining. **d** Similarly, the localization of the XY body (*arrow*) is not discernible by DAPI staining and requires colocalization with the signal obtained by FISH using a horse-specific X chromosome probe (*red*). *Arrowheads* indicate the position of synapsed bivalents following staining with SMC3 (*green*) during pachytene stage. Scale bar=10  $\mu\text{m}$

territory occupied by the XY body is readily identified by its characteristic DAPI-bright appearance (Fig. 1a, c). However, in horse pachytene spermatocytes, the position of the sex chromosome bivalent was not discernible by DAPI staining alone and detection required FISH analysis using a whole chromosome paint (*red*) specific to the equine X chromosome (Fig. 1b, d). The absence of prominent DAPI-stained heterochromatin domains in pachytene spermatocytes indicates the unique properties of global chromatin organization in equine spermatocyte nuclei and prompted us to conduct a systematic analysis of meiotic sex chromosome inactivation and XY body formation in this species.

The protein complexes associated with synaptonemal complex formation in the equine germ line have not been previously characterized. The use of multiple polyclonal antibodies against SYCP2 and SYCP3 proteins in the horse failed to provide a reliable staining pattern (data not shown), and hence, we set out to identify an alternative meiotic marker for the analysis of homologous chromosome interactions in the horse. Structural maintenance of chromosomes (SMC) is a highly conserved protein family crucial for chromosome remodeling processes (White and Erickson 2006; Jessberger 2002). Importantly, the cohesin subunit SMC3 is known to colocalize with the synaptonemal complex proteins SYCP2/SYCP3 during the pachytene stage of meiosis in the mouse and hence provides a reliable marker for the analysis of chromosome synapsis (Eijpe et al. 2000; Prieto et al. 2004; Revenkova and Jessberger 2006). Consistent with a high degree of homology between mouse and equine *Smc3* coding sequences, *Smc3* transcripts were detected in several equine tissues including testis (T), ovary (Ov), and liver (Li) (Fig. 2a). No amplicons for *Smc3* or the housekeeping gene  $\beta$ -actin were detected in the negative control tissue samples processed in the absence of reverse transcriptase (–RT). These results are consistent with a ubiquitous *Smc3* expression pattern in both the somatic and germ line in the horse.

Simultaneous immunolocalization of centromeres with the CREST antiserum (*red*) as well as meiotic chromosome axes with an anti-SMC3 antibody on surface spread equine spermatocytes revealed that SMC3 (*green*) is an abundant nuclear protein that exhibits a dynamic chromosomal localization throughout the different stages of meiotic prophase I (Fig. 2b). Leptotene stage spermatocytes were easily recognized by the presence of 64 CREST signals with some peripheral centromeric domains likely corresponding to telocentric chromosomes involved in a characteristic bouquet configuration (*arrow*). At this stage, the SMC3 protein exhibits diffuse nucleoplasmic staining and only a limited association with condensing chromosome axes (Fig. 2b, top panel). At the zygotene stage, the



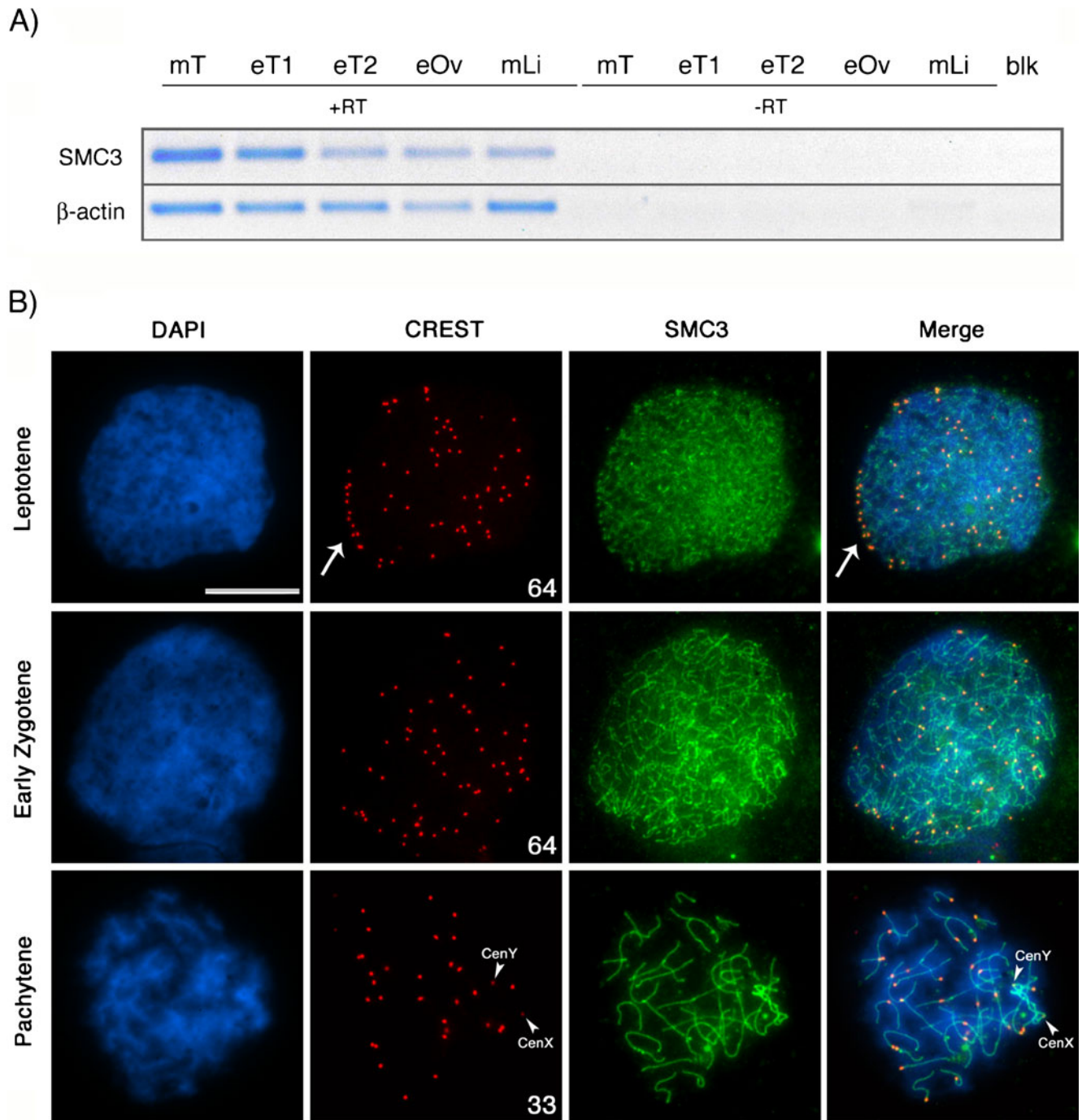


**Fig. 2** Analysis of meiotic configuration in equine spermatocytes. **a** Expression of the structural maintenance of chromosomes 3 (SMC3) coding sequences in mouse (*mT*) and horse (*eT*) testis tissue, equine fetal ovary (*eOv*), and mouse liver tissue (*mLi*) by RT-PCR.  $\beta$ -actin mRNA expression was used as housekeeping control. No amplification was detectable under omission of reverse transcriptase (–RT) or in the negative control (*blk*). **b** Immunochemical localization of kinetochore proteins (CREST, red) and synaptonemal complex components (SMC3, green) in equine spermatocytes reveals the position of the centromere in each of the 64 asynapsed equine

chromosomes during leptotene. Note the arrangement of telocentric chromosome bivalents on a bouquet configuration (arrow, upper panel). At the zygotene stage (middle panel), centromeres become redistributed throughout the nucleoplasm. The number of CREST signals decreases to 33 at the pachytene stage (lower panel), indicating complete synapsis between 31 autosomal chromosome pairs. Pairing of the sex chromosomes, however, remains restricted to a distal pseudoautosomal region and centromeres remain separated as indicated by two smaller CREST foci (CenY and CenX) (lower panel, arrowheads). DNA is shown in blue. Scale bar=10  $\mu$ m

majority of CREST signals disperse throughout the nucleoplasm, and the SMC3 protein exhibits a uniform staining throughout most of the length of the chromosomal axis (middle panel). At pachytene, chromosome synapsis results in the formation of 31 autosomal CREST signals and two unpaired centromeric signals potentially corresponding to the X and the Y chromosomes (arrowheads). At this stage, SMC3-labeled cohesin axes co-localize with the axial elements of the synaptonemal complex in autosomal bivalents therefore providing a reliable marker to determine the extent of chromosome synapsis during prophase I of meiosis in the equine species. Notably, the interstitial segments of the two remaining chromosomes that exhibit unpaired centromeric regions presented a distinctly brighter SMC3 signal compared to the fully synapsed autosomal bivalents in the majority (>95%) of pachytene stage cells evaluated ( $n=103$ ) (Fig. 2b, lower panel). These results provide the first characterization of the dynamics of homologous chromosome synapsis, centromere associations, and chromosomal localization of the SMC3 protein during equine meiosis.

The cohesin subunit SMC3 is enriched at the XY bivalent in equine pachytene stage spermatocytes

To establish whether the SMC3 protein is preferentially enriched at the sex chromosome bivalent, we determined the position of the X chromosome following immunocytochemistry of pachytene stage spermatocytes and the use of whole chromosome probes specific for the X chromosomes. Analysis of mouse pachytene stage spermatocytes revealed subtle differences in the intensity of SMC3 staining between autosomes and the sex chromosome bivalent detected by co-localization with the murine X-chromosome probe (Fig. 3a, top panel). By comparison, immuno-FISH analysis of equine pachytene stage spermatocytes with the equine X chromosome probe revealed a prominent enrichment of SMC3 protein associated with the sex chromosomes in the majority of cells (>90%) evaluated ( $n=35$ ) (Fig. 3a, lower panel). Next, we conducted a quantitative analysis of SMC3 signal intensities of the sex chromosomes compared with two randomly selected autosomal bivalents per nucleus (Fig. 3b). Interestingly, the partially synapsed sex bivalent in equine pachynema exhibited a 1.6-fold higher intensity of SMC3 staining compared to the fully synapsed autosomes ( $p<0.001$ ), while SMC3 labeling intensities in mouse spermatocytes did not show any significant differences ( $p>0.05$ ) between autosomes and gonosomes (Fig. 3b). These results indicate that SMC3 protein exhibits a high affinity for sex chromosome cores in horse spermatocytes and might be associated with yet unidentified features of gonosomal chromatin in the equine species.

$\gamma$ H2AX is preferentially enriched at meiotic sex chromosome cores in equine pachytene spermatocytes

Accumulation of the phosphorylated form of histone H2AX ( $\gamma$ H2AX) is one of the first in a series of histone modifications required for XY body formation and heterochromatinization of this nuclear domain (Fernandez-Capetillo et al. 2003). However, whether  $\gamma$ H2AX is implicated in this process during equine meiosis is not known. Therefore, we determined the patterns of expression and subnuclear localization of  $\gamma$ H2AX in surface spread equine spermatocytes. At the leptotene stage,  $\gamma$ H2AX (red) exhibits a diffuse nuclear localization (Fig. 4a). This pattern is consistent with the formation of multiple double strand DNA breaks (DSBs) reported at this stage during mouse meiosis (Mahadevaiah et al. 2001; Turner et al. 2005). Zygotene stage spermatocytes present a gradual decrease in  $\gamma$ H2AX staining associated with asynapsed chromosomes. As the process of homologous chromosome synapsis ensues and following the resolution of DSBs in pachytene stage spermatocytes,  $\gamma$ H2AX staining becomes restricted to the sex chromosome bivalent. Notably, a direct comparison of the patterns of  $\gamma$ H2AX localization in mouse and equine pachytene spermatocytes (Fig. 4b) revealed that in striking contrast to the mouse spermatocyte in which  $\gamma$ H2AX exhibits a cloud-like staining pattern over a prominent macrochromatin domain (Mahadevaiah et al. 2001),  $\gamma$ H2AX is mainly restricted to SMC3-bright (green) meiotic sex chromosome cores (Fig. 4b).

Next, a non-bias co-localization analysis was conducted using the overlap coefficient ( $R$ ) according to Manders (Zinchuk and Zinchuk 2008), to determine the degree of co-localization between fluorescent signals originating from SMC3 and  $\gamma$ H2AX immunocytochemistry at the nuclear domain occupied by the sex bivalents (Fig. 4c). The co-localization coefficient between SMC3 and  $\gamma$ H2AX in horse pachytene spermatocytes ( $R_{\text{horse}}=0.71$ ) indicates that a significantly larger proportion of the total  $\gamma$ H2AX signal is associated with the chromosome axes (signal overlap with SMC3 is  $50.4\pm 13.9\%$ , Fig. 4d). In striking contrast, more than 80% of the total  $\gamma$ H2AX signal (co-localization coefficient is  $R_{\text{mouse}}=0.46$ ) extends beyond chromosome axes in mouse spermatocytes. These data demonstrate that  $\gamma$ H2AX in the mouse accumulates over the entire heterochromatic macrochromatin domain characteristic of this species, whereas  $\gamma$ H2AX is predominantly associated with meiotic chromosome axes in equine spermatocytes (Supplemental Figure S1a) and does not extend to the entire sex chromatin domain (Supplemental Figure S1c), further suggesting that alternative pathways of XY body formation might be at play in the horse.

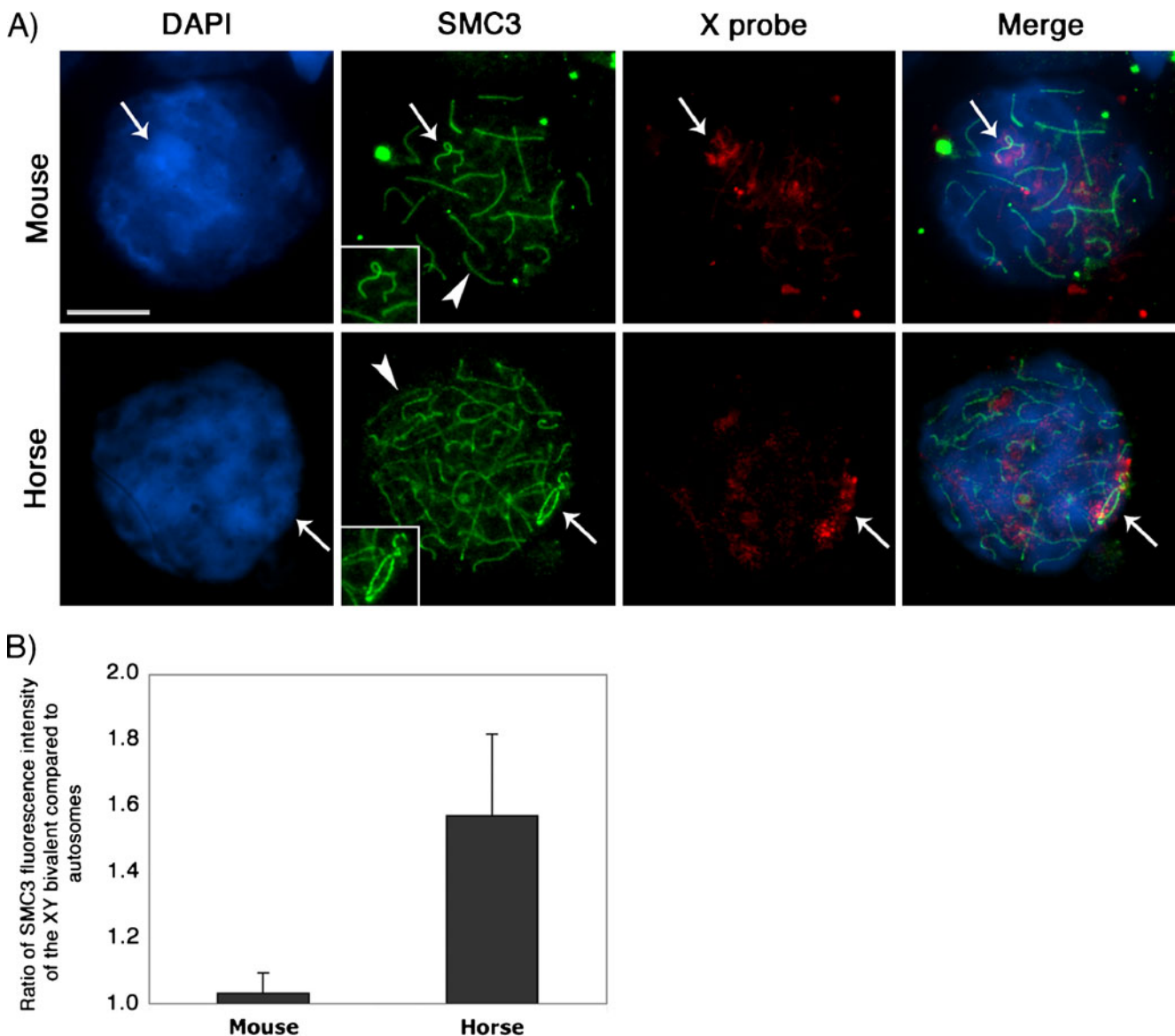


**Fig. 3** The cohesin subunit SMC3 is enriched at the sex chromosome bivalent in equine pachytene spermatocytes. **a** SMC3 (green) marks cohesin axes at synapsed chromosomes (arrowheads) in mouse and horse spermatocytes. In horse nuclei, SMC3 is preferentially enriched at the sex chromosome bivalent (arrow and inset, lower panel) as

evidenced by co-localization with the signal originating from an X chromosome-specific probe (red). DNA is shown in blue. Scale bar=10 $\mu$ m. **b** Ratio of fluorescence intensities at sex chromosome bivalents ( $n=10$  for each species) compared to autosomes in equine and mouse spermatocytes, respectively

#### Lack of repressive chromatin modifications at the equine sex chromosome bivalent

Histone posttranslational modifications play a critical role in the formation, large-scale chromatin remodeling and transcriptional silencing of the XY body in mammals (Mahadevaiah et al. 2001; Fernandez-Capetillo et al. 2003; Hoyer-Fender 2003; Handel 2004; Turner 2007). Importantly, incorporation of histone variants is also an essential mechanism for the process of nucleosome replacement and heterochromatinization of the macrochromatin domain (van der Heijden et al. 2007). However, the types of histone posttranslational

modifications present in the equine XY body and their potential interactions to regulate chromatin structure and function are not known.

Dimethylation of histone H3 on lysine 4 (H3K4me2) is a prominent epigenetic mark that might be important for chromatin remodeling of the sex chromosomes in pachytene stage mouse spermatocytes (Khalil et al. 2004; Khalil and Driscoll 2006). In this species, H3K4me2 seems to be excluded from centromeric heterochromatin domains detected by DAPI staining (Fig. 5a, arrowhead, top panel). However, H3K4me2 (green) associates with autosomal euchromatin and is highly enriched at the sex body where



it is co-localized with  $\gamma$ H2AX (red) over the entire macrochromatin domain (Fig. 5a, arrow). In equine spermatocytes, H3K4me2 exhibits a diffuse nucleoplasmic localization, consistent with the presence of transcriptionally permissive histone modifications at euchromatic domains. Importantly, H3K4me2 is conspicuously absent from the nuclear territory occupied by the XY body, where  $\gamma$ H2AX co-localizes with the sex chromosome cores (Fig. 5a, arrow, lower panel).

Ubiquitination of histone H2A (ubH2A) has also been implicated in the process of heterochromatinization and transcriptional silencing of the XY body as well as transcriptional silencing of asynapsed chromosomes in both the human and mouse germ line (Baarends et al. 1999, 2005). In mouse pachytene spermatocytes, ubH2A (red) exhibits a prominent localization with the macrochromatin domain as well as with telomeric regions of meiotic bivalents (Baarends et al. 1999, 2005; Fig. 5b, arrow). In contrast, in equine spermatocytes, ubH2A (red) is present as a diffuse nucleoplasmic signal and exhibits no evidence for any preferential localization at the sex chromosome bivalent (Fig. 5b, arrow). Although epitope masking at the pachytene stage remains a formal possibility, the patterns of ubH2A staining in the form of distinct telomeric foci in the majority of synapsed autosomal bivalents (arrowheads) as well as the robust nucleoplasmic staining argue against this notion.

Incorporation of the histone variant macroH2A1.2 (H2AFY) into the XY body is a highly dynamic process that might contribute to the transcriptional repression of X- and Y-linked genes. In mouse spermatocytes, it is first detected at the synaptonemal complex at the early pachytene stage and subsequently redistributes to pericentric heterochromatin of autosomes as well as the XY body during mid to late pachytene stage, (Hoyer-Fender et al. 2004; Fig. 5c, arrowhead). At this stage, H2AFY exhibits a precise co-localization with  $\gamma$ H2AX (red) over the entire macrochromatin domain (Fig. 5c, arrow). In contrast, the nuclear localization of H2AFY exhibits marked differences in equine spermatocytes. For example, in this species, H2AFY remains co-localized with the synaptonemal complex during late pachytene stage and exhibits no association with pericentric heterochromatin (Fig. 5c, lower panel). Notably, this histone variant is also co-localized with  $\gamma$ H2AX (red) at meiotic sex chromosome cores (Fig. 5c, arrow). These results provide the first evidence for the existence of unique chromatin modifications at the XY body in equine spermatocytes and suggest that alternative mechanisms might be set in place for the establishment and/or maintenance of specific epigenetic marks at the sex chromatin in this species. Importantly, our data also indicate that H2AFY is a novel member of an as yet to be characterized group of protein complexes

**Fig. 4** Association of  $\gamma$ H2AX with meiotic sex chromosome cores in equine pachytene spermatocytes. **a** During leptotene (*upper panel*) and zygotene (*middle panel*) stages of meiosis,  $\gamma$ H2AX (red) exhibits a diffuse nucleoplasmic staining indicating the presence of DNA double strand breaks. At the pachytene stage,  $\gamma$ H2AX is found associated primarily with sex chromosome cores (*lower panel, arrow*). **b** In contrast to mouse pachytene spermatocytes, which exhibit a prominent, cloud-like, association of  $\gamma$ H2AX with the macrochromatin domain of the XY body (*left image, arrow*), horse pachytene spermatocytes exhibit  $\gamma$ H2AX staining at the sex chromosome cores only (*right image, arrow*). **c** Determination of Mander's colocalization coefficients ( $R$ ) to quantify the levels of  $\gamma$ H2AX staining (red) beyond sex chromosome cores (green) in mouse and horse pachytene spermatocytes. **d** Percentage of signal overlap between  $\gamma$ H2AX and SMC3 at mouse and horse XY bodies ( $n=10$  for each species), demonstrating that  $\gamma$ H2AX staining extends beyond meiotic chromosome cores and occupies the entire macrochromatin domain in the mouse. In striking contrast, a higher degree of co-localization indicates that  $\gamma$ H2AX is essentially restricted to XY chromosome cores in horse pachytene spermatocytes. DNA is shown in blue and SMC3 in green. Scale bar=10  $\mu$ m

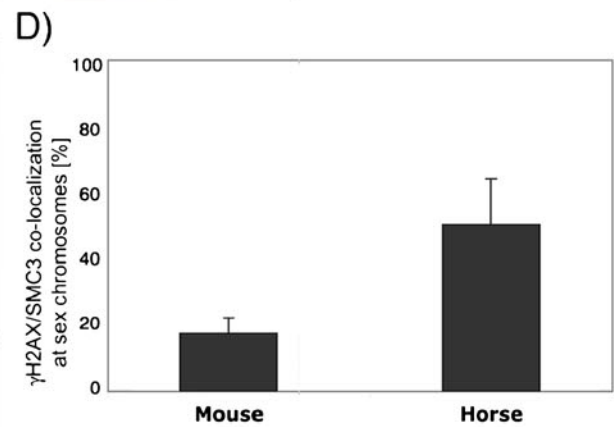
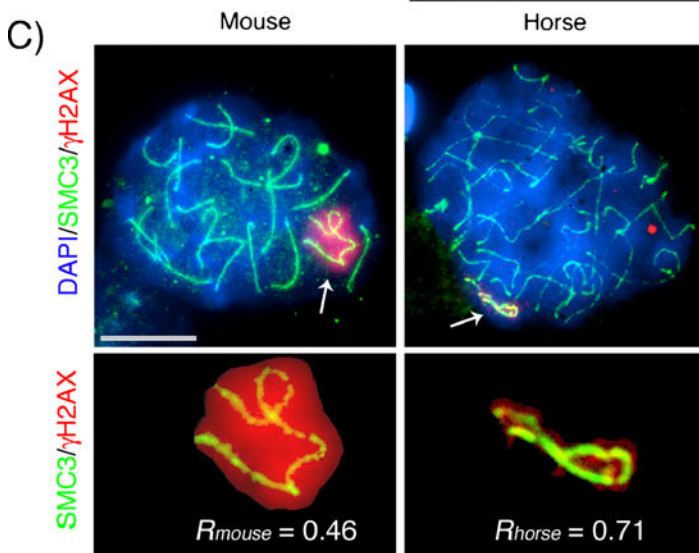
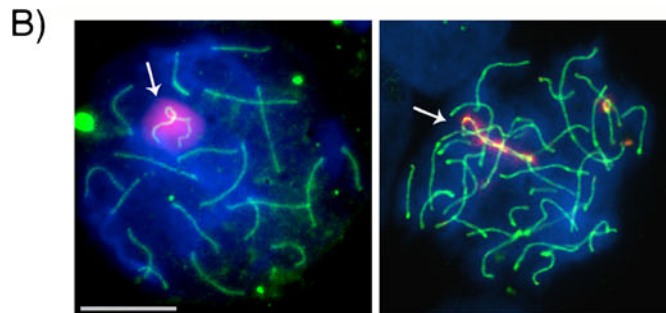
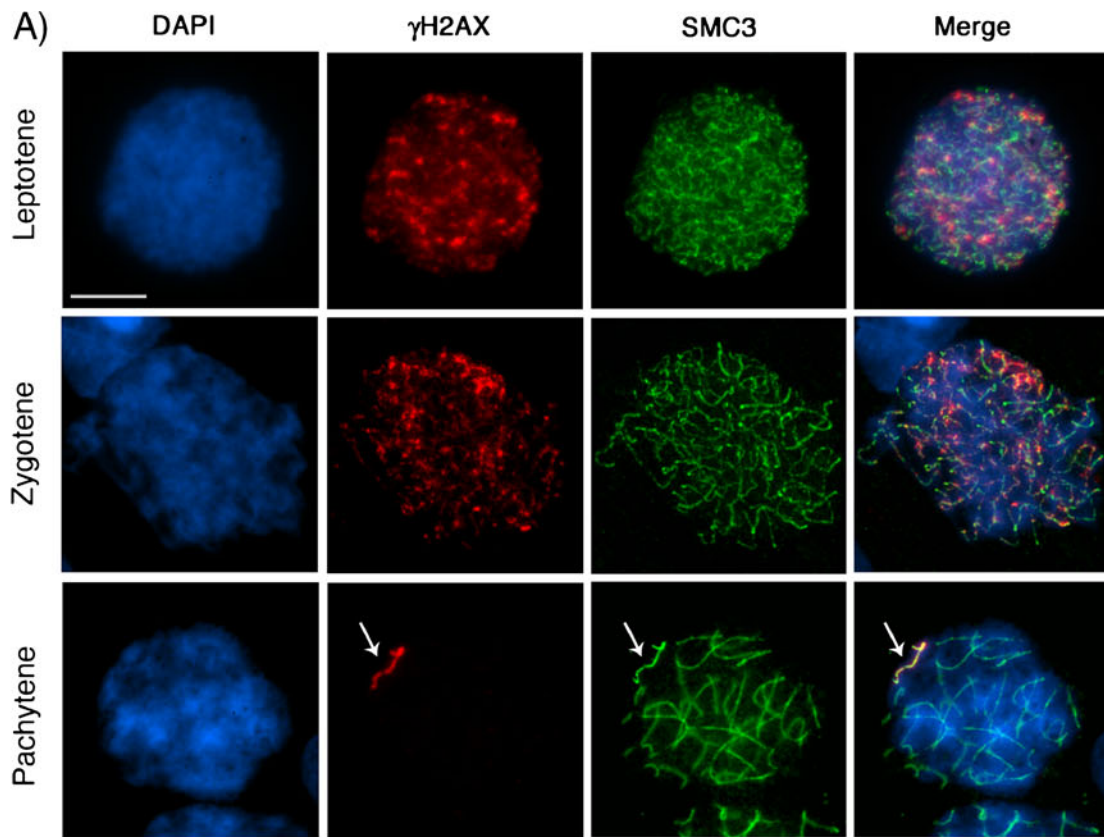
associated with chromatin adjacent with the synaptonemal complex axial cores in horse spermatocytes.

#### Persistence of phosphorylated RNA polymerase II at the XY body in equine spermatocytes

During mid-pachytene stage of meiosis in the mouse, the XY body becomes transcriptionally inactive through the process of MSCI (Handel 2004; Turner et al. 2005; Baarends et al. 2005). Meiotic sex chromosome inactivation is essential for meiotic progression and male fertility and is a complex process that involves large-scale chromatin remodeling as well as the exclusion of RNA polymerase II and splicing factors from the XY body (Monesi 1965; Turner 2007). Therefore, we determined the subnuclear distribution of two component molecules of the basal transcriptional machinery, i.e., RNA polymerase II and the pre-messenger RNA splicing factor Smith antigen, a component of small nuclear ribonucleoproteins involved in RNA processing (Richler et al. 1994).

Similar to the patterns observed in mouse pachytene spermatocytes (Richler et al. 1994; Fig. 6a), Smith antigen (red) was detectable throughout the nucleoplasm of equine spermatocytes, but clearly excluded from the nuclear domain occupied by the X and the Y chromosomes (Fig. 6a, arrow), suggesting that the equine XY bivalent is largely devoid of this element of the splicing machinery. Similarly, RNA polymerase II (Pol II; red) exhibits prominent nucleoplasmic staining but is mostly excluded from the XY body in mouse pachytene spermatocytes (Turner et al. 2005; Baarends et al. 2005; Fig. 6b, top panel), although some residual Pol II expression was detected at the sex body in a small proportion (15%) of mouse spermatocytes (Supplemental Figure S1b). As expected, the nucleoplasm of equine pachytene spermatocytes





cytes was characterized by a diffuse pattern of RNA polymerase II (red), indicating transcriptional activity of the autosomal compartment in this species (Fig. 6b, lower panel). Consistent with our previous experiments, the equine sex chromosome bivalent was easily identified by its preferential enrichment with SMC3 protein (green). Notably, prominent Pol II expression was detected in the form of distinct foci showing a precise co-localization with the sex chromosome cores, in >65% of equine mid-pachytene spermatocytes (Fig. 6b, c, arrowheads, lower panel). In contrast to mouse nuclei, RNA polymerase II was excluded from the territory occupied by the XY body only in approximately 10% of equine spermatocytes. These results indicate that focal associations of RNA polymerase II persist at this nuclear domain and may hence suggest transcriptional activity of specific genomic segments of the XY body in the horse germ line.

#### Chromosomal distribution of recombination events in equine spermatocytes

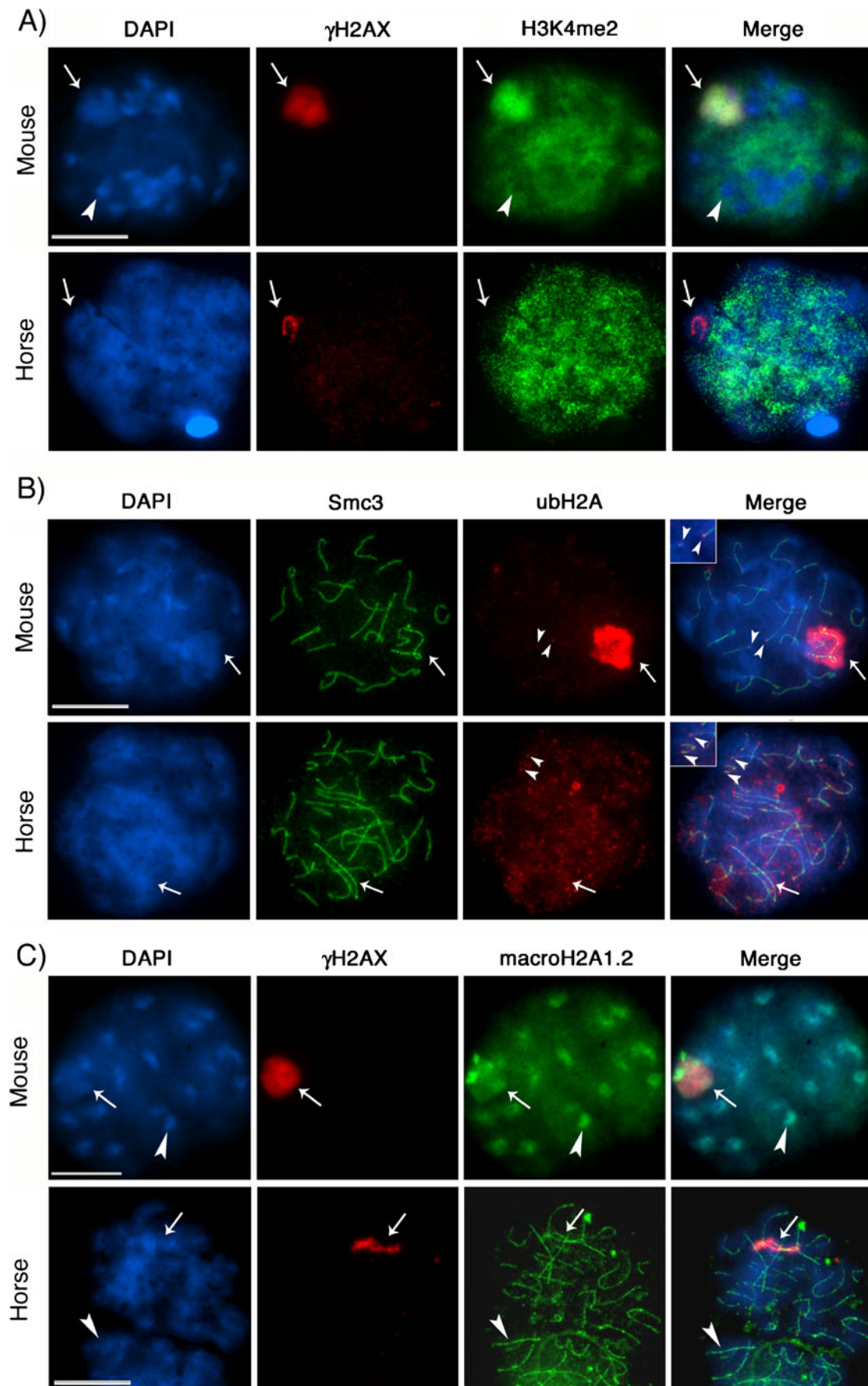
The patterns of SMC3 expression provide a robust and specific marker for the identification of the equine sex chromosome bivalent and hence allow for a high-resolution analysis of the dynamics of pairing events between the X and the Y chromosomes as well as a detailed analysis of the topological distribution of DNA recombination sites. For example, the localization of autosomal and gonosomal centromeric domains can be determined using CREST antiserum, confirming the position of the PAR at the distal portion of the acrocentric Y and the short arm of the submetacentric X chromosome in the horse (Fig. 7a). Next, to provide insight into recombination frequencies in equine spermatocytes, we determined the chromosomal localization of RAD51 and MLH1 proteins. Resolution of DSBs is marked by disappearance of RAD51 foci from fully synapsed bivalents in mouse pachytene spermatocytes (Bannister and Schimenti 2004; Burgoyne et al. 2007). In contrast, RAD51 foci persist in the synapsed chromosomes from equine spermatocytes at the early to mid-pachytene stage and become resolved only by the diplotene stage (Fig. 7b and Supplemental Figure S1d). The mismatch repair protein MLH1 is a component of mature recombination nodules at synaptonemal complexes during late pachytene stage of meiosis (Anderson et al. 1998; Froenicke et al. 2002). However, no information is available concerning the chromosomal distribution of MLH1 foci in the equine species. Our results indicate that each synapsed bivalent in late pachytene stage nuclei is characterized by the presence of 1 or 2 distinct MLH1 foci (red), indicating the presence of an average of  $1.64 \pm 0.06$  crossover events per autosomal bivalent or  $51.97 \pm 1.86$  foci per nucleus (Fig. 7c, d). Importantly, in the majority of pachytene spermatocytes, a

**Fig. 5** Epigenetic modifications at the sex chromosome bivalent in equine pachytene spermatocytes. **a** Histone H3 dimethylation at lysine 4 (H3K4me2; green) exhibits a diffuse nucleoplasmic staining but is excluded from pericentric heterochromatin domains in mouse pachytene spermatocytes (arrowhead). Note the prominent accumulation of H3K4me2 at the macrochromatin domain and its co-localization with  $\gamma$ H2AX (red) in mouse nuclei (arrow). In contrast, the equine XY body is completely devoid of this histone modification (arrow, lower panel), while the localization to euchromatic domains is conserved. **b** The mono-ubiquitinated form of histone H2A (ubH2A, red) co-localizes with telomeric domains (arrowheads, insets) in mouse (upper panel) and horse (lower panel) pachytene spermatocytes and shows a prominent accumulation at the XY body in the mouse (arrow). In the horse, ubH2A exhibits a diffuse nucleoplasmic staining with no preferential enrichment at sex chromatin (arrow, lower panel). **c** The histone variant macroH2A1.2 (green) is co-localized with  $\gamma$ H2AX (red) at the macrochromatin domain and shows a preferential enrichment at DAPI-bright pericentric heterochromatin (arrowhead) in mouse spermatocytes. In equine spermatocytes, macroH2A1.2 labels lateral elements of the synaptonemal complex in all chromosome bivalents and is exclusively associated chromosome cores at the XY body (arrow). DNA is shown in blue. Scale bars=10  $\mu$ m

single MLH1 focus (arrowhead) is detectable within the PAR of the equine X and Y chromosomes (arrow).

#### Discussion

In the mammalian male germ line, transcriptional repression of X- and Y-linked genes is associated with striking changes in heterochromatinization and large-scale chromatin remodeling at the sex chromosome bivalent resulting in the formation of the XY body (Handel 2004; Turner 2007; Namekawa and Lee 2009). Importantly, formation of this specialized nuclear domain is essential for male fertility in mammals (Fernandez-Capetillo et al. 2003; Turner 2007). In this study, we provide the first evidence indicating that unique mechanisms are set in place for the control of heterochromatinization and establishment of epigenetic modifications associated with the XY bivalent during equine meiosis (summarized in Fig. 8). Analysis of the kinetics of homologous chromosome synapsis in equine spermatocytes revealed the presence of a characteristic bouquet configuration at the leptotene stage. Notably, the cohesin subunit SMC3 is highly enriched at the sex chromosome bivalent at the mid to late pachytene stage where  $\gamma$ H2AX is found primarily associated with the X and Y chromosome cores. In striking contrast with the XY body of the mouse, macroH2A1.2 remains restricted to a region closely circumscribing the chromosome axes at the equine XY body. Moreover, transcriptionally repressive chromatin modifications such as ubH2A and histone modifications associated with major chromatin remodeling such as H3K4me2 are conspicuously absent from the sex chromosome bivalent. Interestingly, the absence of these hetero-





chromatin marks is also associated with persistence of RNA polymerase II foci at the sex chromosomes. Collectively, our results indicate that consistent with its critical role in XY body formation,  $\gamma$ H2AX is a prominent, if spatially restricted, mark at this nuclear domain in equine pachytene stage spermatocytes. Taken together, our results indicate that sex chromatin in the horse exhibits a unique epigenetic landscape reminiscent of a transcriptionally permissive chromatin environment.

#### Homologous chromosome synapsis and meiotic recombination in equine spermatocytes

In contrast to the rapid advances in sequencing the horse genome (Wade et al. 2009), only limited information is currently available on the process of meiosis in this species. Pioneering studies used air-dried chromosomal spreads to describe the meiotic chromosomes of equine interspecific hybrids as well as the number of chiasmata during normal meiosis in the stallion (Chandley et al. 1974; Scott and Long 1980). A subsequent study used electron microscopy for the analysis of synaptic abnormalities in a horse carrying an autosomal trisomy (Power et al. 1992). However, neither the behavior of centromeres nor the kinetics of homologous chromosome synapsis in the equine germ line has been previously documented. Identification of the bouquet configuration in equine spermatocytes at the leptotene stage is consistent with the notion that some topological features of telomere/centromere redistribution during early meiosis have been highly conserved in mammals and that this structure is important for homologous chromosome search and synapsis (Scherthan 2001). Contrary to other species, however, centromeres of fully synapsed equine chromosomes remain dispersed throughout the nucleus at the pachytene stage and might account for the absence of large blocks of centromeric heterochromatin at this stage. Therefore, it is conceivable that the lack of heterochromatic block formation in equine pachytene stage spermatocytes might be linked to this unusual type of centromere dynamics.

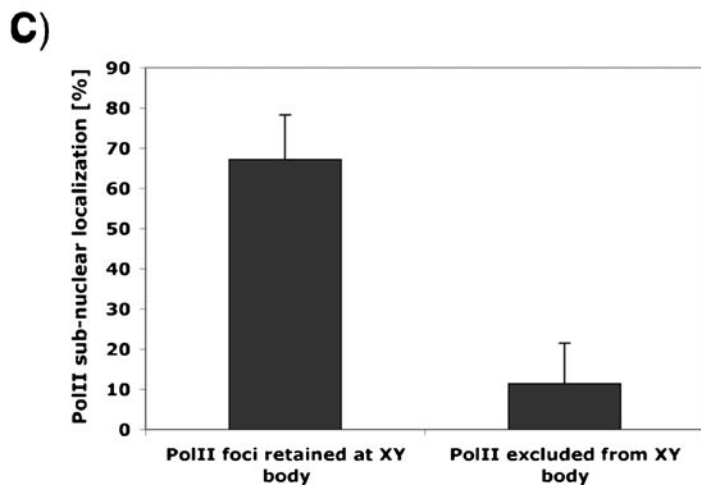
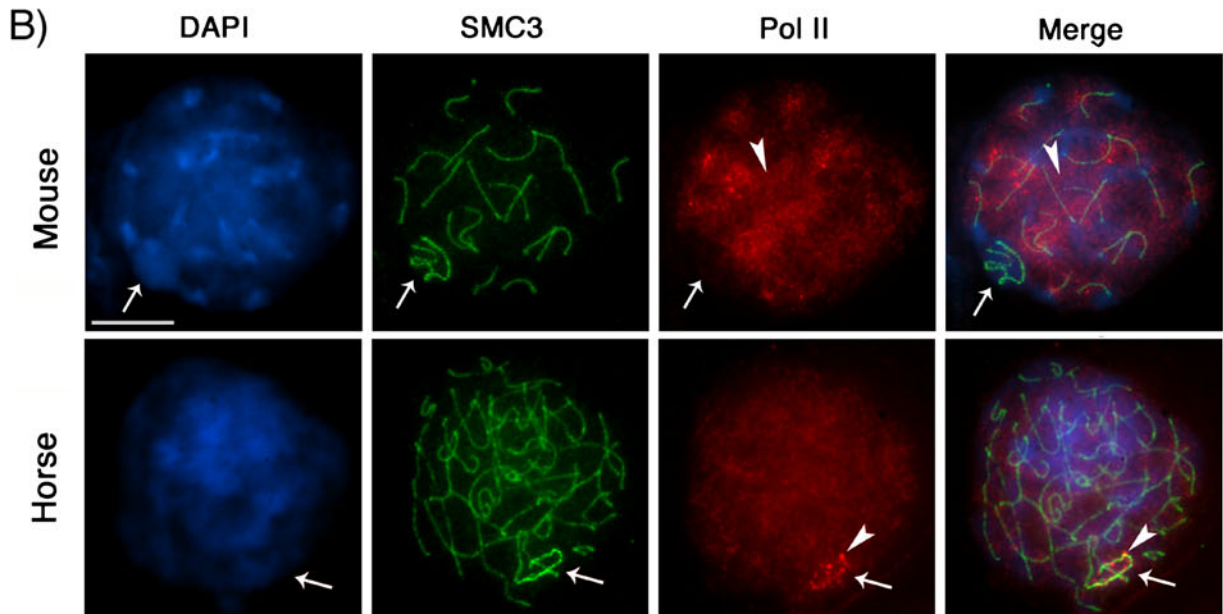
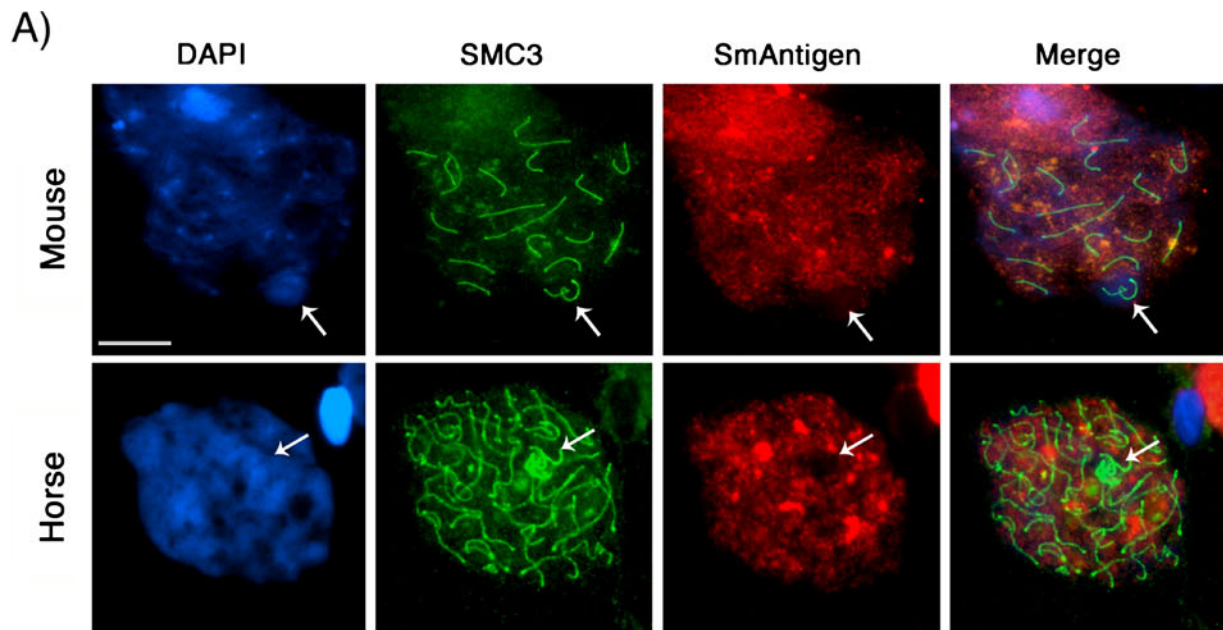
The SMC3 protein has a structural role in chromosome compaction, assembly of the synaptonemal complex, and recruitment of recombination factors (Revenkova and Jessberger 2006; Peltari et al. 2001). Consistent with its prominent role during mammalian meiosis, SMC3 is an abundant nuclear protein in equine spermatocytes that becomes progressively associated with meiotic chromosome axes and, by the pachytene stage, is predominantly decorating chromosome cores at synapsed bivalents. Subtle, albeit potentially important, differences in the patterns of SMC3 chromosomal localization seem to exist among different species. For example, the levels of SMC3 protein are low during the leptotene and zygotene stages in rat

**Fig. 6** Persistence of RNA polymerase II at the XY body in equine spermatocytes. **a** The pre-messenger RNA splicing factor Smith antigen (red) is present in the nucleoplasm of mouse (upper panel) and horse (lower panel) spermatocytes, but is excluded from the XY body in both species (arrow). **b** RNA polymerase II (red) exhibits a diffuse nucleoplasmic staining in mouse (arrowhead, upper panel) and horse (lower panel) pachytene spermatocytes. In mouse spermatocytes, RNA polymerase II is excluded from the XY body (arrow) in the majority of cells, which is consistent with global transcriptional silencing of this chromatin domain. In contrast, RNA polymerase II foci (arrowhead) persist associated with sex chromosome cores in equine spermatocytes **c** Proportion of equine spermatocytes with RNA polymerase II staining. DNA is shown in blue. Scale bar=10  $\mu$ m

spermatocytes and subsequently increase at the pachytene and diplotene stages (Eijpe et al. 2000). In addition, SMC3 seems to co-localize with axial elements on a “beads on a string pattern”, whereas in equine pachytene spermatocytes, SMC3 protein decorates the entire length of meiotic chromosome cores. Similar to the mouse (Prieto et al. 2004), SMC3 staining is present from the leptotene stage in equine spermatocytes and becomes associated with entire chromosome axes at the zygotene stage, perhaps reflecting structural differences in chromosome axis formation and/or condensation among different species (Prieto et al. 2004; Revenkova and Jessberger 2006). In support of this hypothesis, our study also revealed a striking enrichment of SMC3 at the sex chromosome bivalent reminiscent of axial thickening at sex chromosomes as previously observed by electron microscopy in equine spermatocytes (Power et al. 1992; Solari 1970a, b; Tres 1977). In addition, differential associations of cohesin subunits with sex chromosome cores have been reported in mice and marsupials (de la Fuente et al. 2007; Page et al. 2006). Although this is the first report of SMC3 enrichments on sex chromosome axes during equine spermatogenesis, the mechanisms and functional implications of SMC3 accumulation at the equine XY body are not clear at present. However, it might signal the presence of unique chromatin remodeling events at this nuclear domain, or alternatively, it might reflect the affinity of SMC3 for palindromic DNA (Akhmedov et al. 1999; Hawley 2003).

Our results are consistent with previous studies indicating the terminal associations between the distal segment of the acrocentric Y and the short arm of the submetacentric X chromosome to form the pseudoautosomal region in the horse (Scott and Long 1980; Power et al. 1992). However, our study provides critical insight into the frequency and chromosomal distribution of recombination events in the equine species. Interestingly, RAD51 foci persist in the synapsed chromosomes of early to mid-pachytene stage spermatocytes indicating that resolution of DSBs is somewhat delayed compared to the mouse. To our knowledge, this is the first report demonstrating the applicability of meiotic and chromosomal markers for the analysis of chromosome synapsis (SMC3,  $\gamma$ H2AX) and homologous





recombination (Rad51, MLH1) in the horse. Further studies, however, are required to determine the kinetics of the RAD51 pathway as well as any potential function(s) of SMC3 in the assembly of recombination complexes during equine meiosis.

$\gamma$ H2AX is a prominent marker of meiotic sex chromosome cores in equine spermatocytes

The presence of abundant nucleoplasmic  $\gamma$ H2AX staining during leptotene and zygotene suggests that some aspects of the regulatory pathways leading to  $\gamma$ H2AX associations with DSB repair and recombination appear to be conserved in the equine species. Importantly, and consistent with its critical role for MSCI in mammals,  $\gamma$ H2AX disappears from the nucleoplasm by the late zygotene stage and becomes exclusively associated with the XY body in equine pachytene spermatocytes. However, in contrast to the majority of mammalian species studied to date,  $\gamma$ H2AX is found primarily associated with the X and Y chromosome cores. Notably, these patterns of chromosomal  $\gamma$ H2AX localization have also recently been described in the female heterogametic avian sex chromosome bivalent (Schoenmakers et al. 2009). Therefore, together with recent observations in chicken sex chromosomes, our results provide additional evidence for marked variations in the patterns of  $\gamma$ H2AX association with the XY body during MSCI. Phosphorylation of histone H2AX might provide one of the earliest signals for MSCI by recruiting chromatin repressive marks such as macroH2A1.2 (Fernandez-Capetillo et al. 2003; Hoyer-Fender et al. 2000; Escalier and Garchon 2000) to the macrochromatin domain of the mouse XY body. The mechanisms underlying large-scale chromatin remodeling at the sex bivalent in the horse are not clear at present. However, results indicate the involvement of different strategies for heterochromatin formation and spreading of epigenetic marks during equine meiosis.

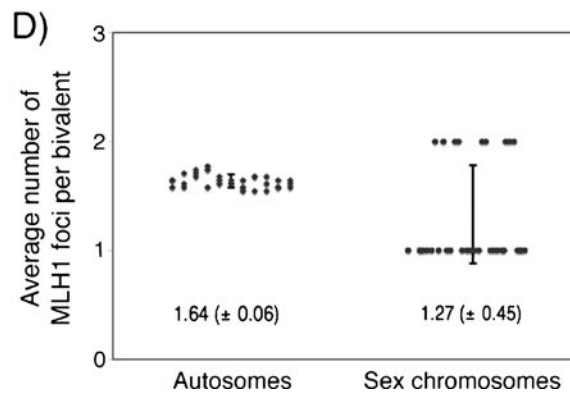
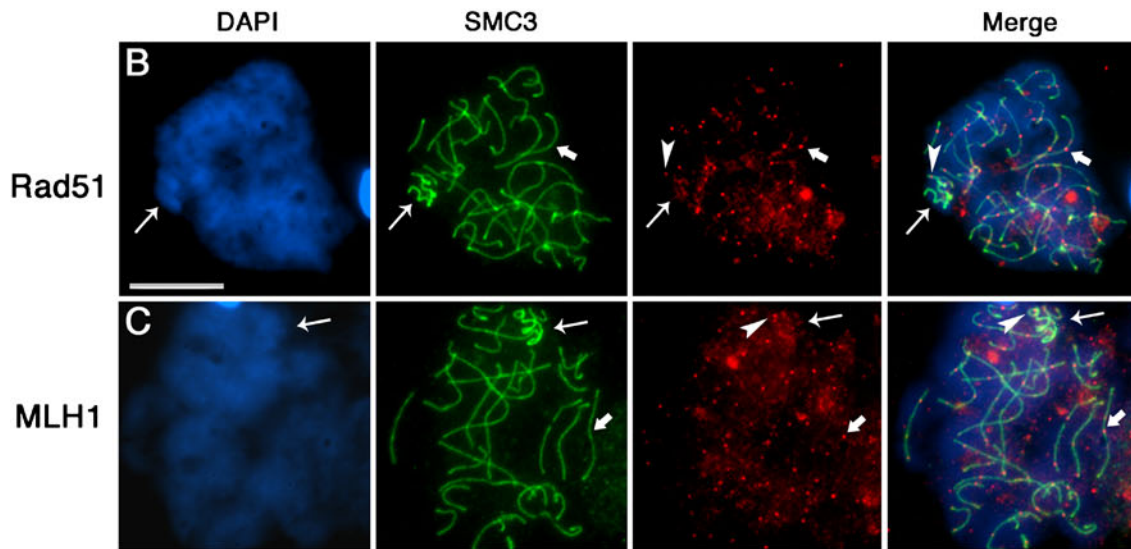
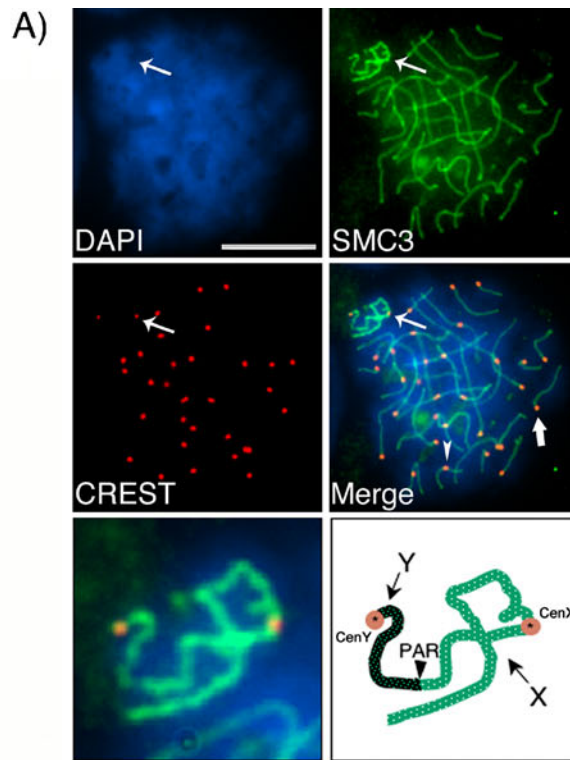
The sex chromosome bivalent exhibits a unique chromatin configuration and epigenetic landscape during equine meiosis

The study of XY body formation during equine spermatogenesis provides a unique experimental paradigm to determine the role of specific epigenetic marks on heterochromatinization and to determine whether establishment of a macrochromatin domain at the XY body is required for transcriptional silencing during MSCI. For example, H3K4me2, a histone modification involved in chromatin remodeling of the murine sex chromosomes (Khalil et al. 2004; Khalil and Driscoll 2006) is conspicuously absent from the XY body in equine pachytene spermatocytes. Further studies are required to determine whether lack of

**Fig. 7** Detection of meiotic recombination events in equine spermatocytes. **a** Simultaneous staining of CREST (*red*) and SMC3 (*green*) reveals the presence of fully synapsed acrocentric and submetacentric bivalents at the pachytene stage. Note that centromeric domains are distributed throughout the nucleoplasm. The pseudoautosomal region (*PAR*) is established between the distant segments of an acrocentric Y chromosome (*dark green* in diagram) and the submetacentric X chromosome (*light green*). The position of the sex chromosome centromeres (CenY and CenX) is indicated. **b** Rad51 foci (*red*) are detected in early pachytene spermatocytes. Each bivalent exhibits one to two Rad51 foci along the chromosome axes (*bold arrow*). The sex chromosomes (*arrow*) exhibit a single Rad51 focus at the PAR (*arrowhead*). **c** The mismatch repair protein MLH1 (*red*) marks the sites of crossover formation along chromosome cores of all autosomes (*bold arrow*). Moreover, the partially synapsed sex chromosomes (*arrow*) show a single MLH1 focus in the majority of cells (*arrowhead*). Scale bar=10  $\mu$ m. **d** Scatter plot diagram to visualize the average numbers of MLH foci per chromosome bivalent ( $2n=64$ ) detected in equine pachytene spermatocytes ( $n=33$ ). DNA is shown in blue. Scale bar=10  $\mu$ m

H3K4me2 is a cause or a consequence of the lack of macrochromatin formation in equine spermatocytes. However, to our knowledge, this is the first demonstration of the lack of H3K4me2 at the equine sex chromosome bivalent, a chromatin mark that has been associated with sex body formation in both marsupials and eutherian mammals alike (Khalil et al. 2004; Khalil and Driscoll 2006; Namekawa et al. 2007). MacroH2A1.2 (H2AFY), a histone variant known to be essential to recruit remodeling complexes required for heterochromatinization during mouse meiosis (Hoyer-Fender et al. 2004), is found exclusively associated with meiotic chromosome cores in equine pachytene spermatocytes. Localization of macroH2A1.2 to filamentous structures reminiscent of the synaptonemal complex has previously been observed in mouse spermatocytes during early pachytene stage. However, in the mouse, this localization pattern was always concomitant with macroH2A1.2 accumulation at the macrochromatin domain of the sex body (Hoyer-Fender et al. 2004). Notably, ubiquitinated histone H2A (ubH2A), a histone modification associated with transcriptional repression (Baarends et al. 1999; Baarends et al. 2005), fails to accumulate at the sex chromosome bivalent in equine spermatocytes suggesting the absence of essential transcriptionally repressive chromatin marks.

Differences in the epigenetic profile of sex chromatin have also been recently described in the opossum (Namekawa et al. 2007) where dimethylation of H3K9 was absent from spermatids and  $\gamma$ H2AX persisted to the secondary spermatocyte stage and in some instances to a small percentage of round spermatids. Therefore, although the basic mechanism of MSCI and transcriptional silencing seems to be conserved from marsupials to mammals, there seem to be variations to this theme in the form of differences in the epigenetic profile and chromatin domains established by the sex chromosomes.





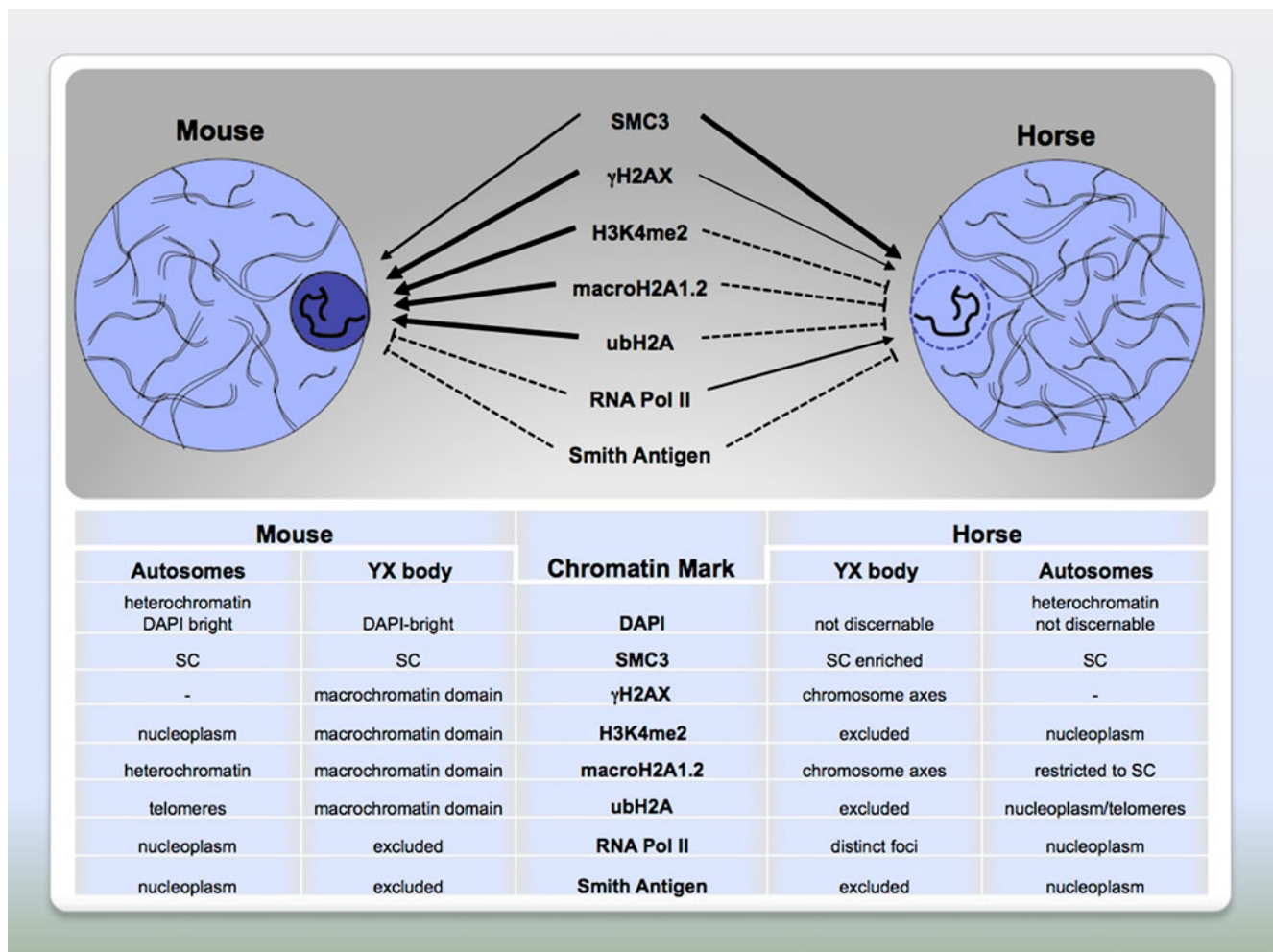


**Fig. 8** Comparison of epigenetic modifications at the XY body in mouse and equine pachytene spermatocytes. The chromatin domain at the XY body in equine pachytene spermatocytes demonstrates evolutionary divergence in both, morphological appearance and in

regard to its epigenetic landscape. *Solid arrows* indicate enrichment; *broken lines* designate absence of enrichment or exclusion from the XY body domain

The presence of a unique epigenetic landscape consistent with a transcriptionally permissive chromatin environment at the equine sex chromosome bivalent might, at least in part, explain the persistence of distinct RNA Pol II foci at the sex chromatin in equine pachytene and diplotene spermatocytes. Interestingly, the active subunit of RNA polymerase II has been recently observed at several discrete regions of the mouse X and Y chromosomes suggesting the presence of chromosomal segments that escape MSC1 in the male germ line (Khalil and Driscoll 2007). Whether RNA Pol II foci at equine sex chromosome cores correlate with sites of active transcription remains to be determined. The equine XY body is clearly devoid of the pre-messenger RNA splicing factor Smith antigen, indicating that the sex chromosomes exhibit to some degree global transcriptional inactivation and lack of mRNA processing during equine spermatogenesis. Further analysis of sex chromatin in the horse will be required to determine the hierarchy of events

leading towards the establishment of specific epigenetic modifications and provide insight into their functional implications for XY body formation and MSC1 in the horse.

Collectively, our results suggest that the epigenetic mechanisms leading to MSC1 differ to some extent among mammalian species. Specifically, we provide the first evidence indicating that unique pathways of histone modifications and chromosomal distribution of histone variants regulate the establishment of epigenetic marks at the XY bivalent. Therefore, some features of XY body formation may be evolutionarily divergent in the domestic horse. It is well established that the Equidae family exhibits one of the fastest rates of karyotypic evolution among mammals, and this process has been linked to high frequencies of centromere repositioning and, ultimately, unique mechanisms in heterochromatin formation (Wichman et al. 1991; Piras et al. 2009; Wade et al. 2009). Therefore, a diverging epigenetic landscape at the XY body in the horse could arise from



such unique heterochromatinization pathways and may provide a valuable model system to further our understanding of heterochromatin formation mechanisms in the mammalian genome.

**Acknowledgments** We thank Dr. W. Earnshaw for the generous gift of human CREST antiserum and Drs. Michaela Kristula and Lauren Greene (Department of Clinical Studies, University of Pennsylvania) for providing equine testicular tissue. We are grateful to E. Amenkhiyan for helping with preliminary data collection and to Dr. M.A. Handel for comments and critical reading of the manuscript. This research was supported by research grants from the University of Pennsylvania Research Foundation and the National Institutes of Health NIH 2RO1HD042740 to R. De La Fuente. The support from McCabe Foundation (M. M. Viveiros) and the Havemeyer Foundation to S. M. McDonnell is also acknowledged.

## References

- Akhmedov A, Gross B, Jessberger R (1999) Mammalian smc3 c-terminal and coiled-coil protein domains specifically bind palindromic DNA, do not block DNA ends, and prevent DNA bending. *J Biol Chem* 274(53):38216–38224
- Anderson SF, Schlegel BP, Nakajima T, Wolpin ES, Parvin JD (1998) BRCA1 protein is linked to the RNA polymerase II holoenzyme complex via RNA helicase A. *Nat Genet* 19:254–256
- Baarends W, Hoogerbrugge J, Roest H, Ooms M, Vreeburg J, Hoeijmakers J, Grootegoed J (1999) Histone ubiquitination and chromatin remodeling in mouse spermatogenesis. *Dev Biol* 207(2):322–333
- Baarends W, Wassenaar E, van der Laan R, Hoogerbrugge J, Sleddens-Linkels E, Hoeijmakers J, de Boer P, Grootegoed J (2005) Silencing of unpaired chromatin and histone H2A ubiquitination in mammalian meiosis. *Mol Cell Biol* 25(3):1041–1053
- Bannister L, Schimenti J (2004) Homologous recombinational repair proteins in mouse meiosis. *Cytogenet Genome Res* 107(3–4):191–200
- Burgoyne P, Mahadevaiah S, Turner J (2007) The management of DNA double-strand breaks in mitotic G(2), and in mammalian meiosis viewed from a mitotic G(2) perspective. *Bioessays* 29(10):974–986
- Burgoyne P, Mahadevaiah S, Turner J (2009) The consequences of asynapsis for mammalian meiosis. *Nat Rev Genet* 10(3):207–216
- Chandley A, Jones R, Dott H, Allen W, Short R (1974) Meiosis in interspecific equine hybrids. I. The male mule (*Equus asinus* × *E. caballus*) and hinny (*E. caballus* × *E. asinus*). *Cytogenet Cell Genet* 13(4):330–341
- De La Fuente R, Viveiros M, Burns K, Adashi E, Matzuk M, Eppig J (2004) Major chromatin remodeling in the germinal vesicle (GV) of mammalian oocytes is dispensable for global transcriptional silencing but required for centromeric heterochromatin function. *Dev Biol* 275(2):447–458
- De La Fuente R, Baumann C, Fan T, Schmidtman A, Dobrinski I, Muegge K (2006) Lsh is required for meiotic chromosome synapsis and retrotransposon silencing in female germ cells. *Nat Cell Biol* 8(12):1448–1454
- de la Fuente R, Parra MT, Viera A, Calvente A, Gomez R, Suja JA, Rufas JS, Page J (2007) Meiotic pairing and segregation of achiasmate sex chromosomes in eutherian mammals: the role of SYCP3 protein. *PLoS Genet* 3(11):e198
- Eijpe M, Heyting C, Gross B, Jessberger R (2000) Association of mammalian SMC1 and SMC3 proteins with meiotic chromosomes and synaptonemal complexes. *J Cell Sci* 113(Pt 4):673–682
- Escalier D, Garchon H (2000) XMR is associated with the asynapsed segments of sex chromosomes in the XY body of mouse primary spermatocytes. *Chromosoma* 109(4):259–265
- Fernandez-Capetillo O, Mahadevaiah S, Celeste A, Romanienko P, Camerini-Otero R, Bonner W, Manova K, Burgoyne P, Nussenzweig A (2003) H2AX is required for chromatin remodeling and inactivation of sex chromosomes in male mouse meiosis. *Dev Cell* 4(4):497–508
- Franco M, Sciarano R, Solari A (2007) Protein immunolocalization supports the presence of identical mechanisms of XY body formation in eutherians and marsupials. *Chromosome Res* 15(6):815–824
- Froenicke L, Anderson L, Wienberg J, Ashley T (2002) Male mouse recombination maps for each autosome identified by chromosome painting. *Am J Hum Genet* 71(6):1353–1368
- Handel MA (2004) The XY body: a specialized meiotic chromatin domain. *Exp Cell Res* 296(1):57–63
- Handel M, Hunt P (1992) Sex-chromosome pairing and activity during mammalian meiosis. *BioEssays* 14(12):817–822
- Hawley RS (2003) The human y chromosome: rumors of its death have been greatly exaggerated. *Cell* 113(7):825–828
- Hoyer-Fender S (2003) Molecular aspects of XY body formation. *Cytogenet Genome Res* 103(3–4):245–255
- Hoyer-Fender S, Singh P, Motzkus D (2000) The murine heterochromatin protein M31 is associated with the chromocenter in round spermatids and is a component of mature spermatozoa. *Exp Cell Res* 254(1):72–79
- Hoyer-Fender S, Czirr E, Radde R, Turner J, Mahadevaiah S, Pehrson J, Burgoyne P (2004) Localisation of histone macroH2A1.2 to the XY-body is not a response to the presence of asynapsed chromosome axes. *J Cell Sci* 117(Pt 2):189–198
- Jessberger R (2002) The many functions of SMC proteins in chromosome dynamics. *Nat Rev Mol Cell Biol* 3(10):767–778
- Khalil AM, Driscoll DJ (2006) Histone H3 lysine 4 dimethylation is enriched on the inactive sex chromosomes in male meiosis but absent on the inactive X in female somatic cells. *Cytogenet Genome Res* 112(1–2):11–15
- Khalil A, Driscoll D (2007) Trimethylation of histone H3 lysine 4 is an epigenetic mark at regions escaping mammalian X inactivation. *Epigenetics* 2(2):114–118
- Khalil AM, Boyar FZ, Driscoll DJ (2004) Dynamic histone modifications mark sex chromosome inactivation and reactivation during mammalian spermatogenesis. *Proc Natl Acad Sci USA* 101(47):16583–16587
- Losada A, Hirano T (2005) Dynamic molecular linkers of the genome: the first decade of SMC proteins. *Genes Dev* 19(11):1269–1287
- Mahadevaiah SK, Turner JM, Baudat F, Rogakou EP, de Boer P, Blanco-Rodriguez J, Jasin M, Keeney S, Bonner WM, Burgoyne PS (2001) Recombinational DNA double-strand breaks in mice precede synapsis. *Nat Genet* 27(3):271–276
- Manders EEM, Verbeek FJ, Aten JA (1993) Measurement of colocalisation of objects in dual-colour confocal images. *J Microsc* 169:375–382
- Monesi V (1965) Differential rate of ribonucleic acid synthesis in the autosomes and sex chromosomes during male meiosis in the mouse. *Chromosoma* 17(1):11–21
- Namekawa SH, Lee JT (2009) XY and ZW: is meiotic sex chromosome inactivation the rule in evolution? *PLoS Genet* 5(5):e1000493
- Namekawa S, VandeBerg J, McCarrey J, Lee J (2007) Sex chromosome silencing in the marsupial male germ line. *Proc Natl Acad Sci USA* 104(23):9730–9735
- Page J, Berrios S, Rufas J, Parra M, Suja J, Heyting C, Fernandez-Donoso R (2003) The pairing of X and Y chromosomes during meiotic prophase in the marsupial species *Thylamys elegans* is maintained by a dense plate developed from their axial elements. *J Cell Sci* 116(3):551–560

- Page J, de la Fuente R, Gómez R, Calvente A, Viera A, Parra M, Santos J, Berríos S, Fernández-Donoso R, Suja J, Rufas J (2006) Sex chromosomes, synapsis, and cohesins: a complex affair. *Chromosoma* 115(3):250–259
- Pelttari J, Hoja M, Yuan L, Liu J, Brundell E, Moens P, Santucci-Darmanin S, Jessberger R, Barbero J, Heyting C, Hoog C (2001) A meiotic chromosomal core consisting of cohesin complex proteins recruits DNA recombination proteins and promotes synapsis in the absence of an axial element in mammalian meiotic cells. *Mol Cell Biol* 21(16):5667–5677
- Perry J, Palmer S, Gabriel A, Ashworth A (2001) A short pseudoautosomal region in laboratory mice. *Genome Res* 11(11):1826–1832
- Piras F, Nergadze S, Poletto V, Cerutti F, Ryder O, Leeb T, Raimondi E, Giulotto E (2009) Phylogeny of horse chromosome 5q in the genus *Equus* and centromere repositioning. *Cytogenet Genome Res* 126(1–2):165–172
- Power M, Gustavsson I, Switonski M, Ploen L (1992) Synaptonemal complex analysis of an autosomal trisomy in the horse. *Cytogenet Cell Genet* 61(3):202–207
- Prieto I, Tease C, Pezzi N, Buesa JM, Ortega S, Kremer L, Martinez A, Martinez AC, Hulten MA, Barbero JL (2004) Cohesin component dynamics during meiotic prophase I in mammalian oocytes. *Chromosome Res* 12(3):197–213
- Revenkova E, Jessberger R (2006) Shaping meiotic prophase chromosomes: cohesins and synaptonemal complex proteins. *Chromosoma* 115(3):235–240
- Richler C, Ast G, Goitein R, Wahrman J, Sperling R, Sperling J (1994) Splicing components are excluded from the transcriptionally inactive XY body in male meiotic nuclei. *Mol Biol Cell* 5(12):1341–1352
- Scherthan H (2001) A bouquet makes ends meet. *Nat Rev Mol Cell Biol* 2(8):621–627
- Schoenmakers S, Wassenaar E, Hoogerbrugge J, Laven J, Grootegoed J, Baarends W (2009) Female meiotic sex chromosome inactivation in chicken. *PLoS Genet* 5(5):e1000466
- Sciurano R, Rahn M, Rey-Valzacchi G, Solari A (2007) The asynaptic chromatin in spermatocytes of translocation carriers contains the histone variant gamma-H2AX and associates with the XY body. *Hum Reprod* 22(1):142–150
- Scott I, Long S (1980) An examination of chromosomes in the stallion (*Equus caballus*) during meiosis. *Cytogenet Cell Genet* 26(1):7–13
- Solari A (1970a) The behaviour of chromosomal axes during diplotene in mouse spermatocytes. *Chromosoma* 31(2):217–230
- Solari A (1970b) The spatial relationship of the X and Y chromosomes during meiotic prophase in mouse spermatocytes. *Chromosoma* 29(2):217–236
- Tres LL (1977) Extensive pairing of the XY bivalent in mouse spermatocytes as visualized by whole-mount electron microscopy. *J Cell Sci* 25(1):1–15
- Turner JM (2007) Meiotic sex chromosome inactivation. *Development* 134(10):1823–1831
- Turner J, Aprelikova O, Xu X, Wang R, Kim S, Chandramouli G, Barrett J, Burgoyne P, Deng C (2004) BRCA1, histone H2AX phosphorylation, and male meiotic sex chromosome inactivation. *Curr Biol* 14(23):2135–2142
- Turner J, Mahadevaiah S, Fernandez-Capetillo O, Nussenzweig A, Xu X, Deng C, Burgoyne P (2005) Silencing of unsynapsed meiotic chromosomes in the mouse. *Nat Genet* 37(1):41–47
- Turner JM, Mahadevaiah SK, Ellis PJ, Mitchell MJ, Burgoyne PS (2006) Pachytene asynapsis drives meiotic sex chromosome inactivation and leads to substantial postmeiotic repression in spermatids. *Dev Cell* 10(4):521–529
- van der Heijden GW, Derijck AA, Posfai E, Giele M, Pelczar P, Ramos L, Wansink DG, van der Vlag J, Peters AH, de Boer P (2007) Chromosome-wide nucleosome replacement and H3.3 incorporation during mammalian meiotic sex chromosome inactivation. *Nat Genet* 39(2):251–258
- Wade C, Giulotto E, Sigurdsson S, Zoli M, Gnerre S et al (2009) Genome sequence, comparative analysis, and population genetics of the domestic horse. *Science* 326(5954):865–867
- White GE, Erickson HP (2006) Sequence divergence of coiled coils—structural rods, myosin filament packing, and the extraordinary conservation of cohesins. *J Struct Biol* 154(2):111–121
- Wichman H, Payne C, Ryder O, Hamilton M, Maltbie M, Baker R (1991) Genomic distribution of heterochromatic sequences in equids: implications to rapid chromosomal evolution. *J Hered* 82(5):369–377
- Xu X, Aprelikova O, Moens P, Deng C, Furth P (2003) Impaired meiotic DNA-damage repair and lack of crossing-over during spermatogenesis in BRCA1 full-length isoform deficient mice. *Development* 130(9):2001–2012
- Zickler D (2006) From early homologue recognition to synaptonemal complex formation. *Chromosoma* 115(3):158–174
- Zinchuk V, Zinchuk O (2008) Quantitative colocalization analysis of confocal fluorescence microscopy images. *Curr Protoc Cell Biol* 39:4.19.1–4.19.16
- Zinchuk V, Zinchuk O, Okada T (2007) Quantitative colocalization analysis of multicolor confocal immunofluorescence microscopy images: pushing pixels to explore biological phenomena. *Acta Histochem Cytochem* 40:101–111